Pergamon

Int. J. Heat Mass Transfer. Vol. 41, No. 3, pp. 653–661, 1998

Printed in Great Britain
0017-9310/98 $19.00+0.00

PII: S0017-9310(97)00186-5

Mechanisms of unsteady mixing of heat carrier with its flowrate variation and flow swirling—II. Results and analysis

B. V. DZYUBENKO, G. A. DREITSER and A. V. KALYATKA
Moscow Aviation Institute, 125871 Moscow, Russia

(*Received* 26 *December* 1995)

Abstract—The results of study of heat carrier mixing for different types of hydrodynamic unsteadiness in helical tube bundles are generalized and analyzed. New generalizing relations are proposed for calculation of unsteady effective turbulent transfer coefficients that can be used to close the initial systems of equations. Deviations of the numerical values of unsteady transfer coefficients from their quasi-steady values are found and explained by the disturbance of the balance among the energy supplied to the flow, turbulent diffusion and turbulence energy dissipation that cause the turbulent flow structure to vary with time.

1. INTRODUCTION

Part 1 of the present article [1] is devoted to considering the theoretical flow model in bundles of helical oval tubes and fuel element. This model is described by a system of equations that can be solved numerically for different types of hydrodynamic unsteadiness. For the system of the initial equations to be closed for the considered cases of heat carrier flowrate increase and decrease, effective turbulent transfer coefficients must be determined from experiment. At the same time, the method of heat diffusion from a group of line heat sources is used for determination of those coefficients. The methods of computational and experimental study of unsteady processes and the experimental setup, on which experiments have been conducted, are examined in ref. [1]. The results of numerical computation of transient processes occurring in the nuclear reactor of the power propulsion plant (NPPP) are also presented in ref. [1].

The objective of this part of the article is to generalize and analyse the results of investigation of unsteady mixing of heat carrier with its flowrate varying in time as well as to obtain new closing empirical relations for calculation of effective turbulent heat and momentum transfer coefficients for different types of hydrodynamic unsteadiness. In this case, the dependences of the transfer coefficients on the determining similarity numbers allow effective turbulent thermal conductivity and viscosity coefficient to be found in terms of the local flow parameters and heat release when unsteady thermal and hydraulic problems [2–5] are solved. The present part is also aimed at explaining the physical nature of deviations of numerical values of unsteady transfer coefficients from their quasi-steady values. These deviations are attributed both to the disturbance of the balance among the energy supplied to the turbulent flow, turbulent diffusion and turbulence energy dissipation in unsteady thermal and hydraulic processes and, hence, to the time variation of the turbulent flow structure.

2. TEMPERATURE FIELDS WITH HEAT CARRIER FLOWRATE VARIATION

As already mentioned, the values of the effective turbulent diffusion coefficients were determined for each time moment by comparing the experimental and predicted heat carrier temperatures at the outlet cross-section of the tube bundle. In doing so, a definite value of the coefficient K was ascribed to each experimental point on the plot $T = f(r/r_{\text{bundle}})$ according to the theoretical curves $T = f(K, r/r_{\text{bundle}})$ [2, 5] drawn on this plot. Then, the quantity K was analysed statistically and its mean value, corrected dispersion, and confidence intervals were determined. This method was used to determine the values of the unsteady coefficient K_{un} and its dependence on time for different types of unsteadiness [2–5].

Figure 1 plots the experimental results on the heat carrier temperature fields as time dependences of temperature for the fixed flow points. These dependencies are compared with the theoretical ones for the same points provided that $K_{\text{un}} = K_{\text{qs}}$. As seen from Fig. 1, the experimentally measured temperature at a sharp time increase of heat carrier flowrate at $N = \text{const}$ lies above the predicted one at $K_{\text{un}} = K_{\text{qs}}$. This points to the decrease in the mixing intensity of heat carrier at the first time moments. This effect can be explained by the decrease of the turbulence intensity in the time-dependent accelerating flow, which is also characteristic of the accelerating spatial flow with the adverse velocity gradient in the flow direction.

NOMENCLATURE

a	thermal diffusivity
c	heat capacity
d	maximum size of the tube oval
d_{eq}	equivalent diameter
d_{bundle}	bundle diameter, $d_{bundle} = 2r_{bundle}$
F	cross-sectional area of the tubes of a bundle
F_f	cross-sectional area of the tube bundle occupied by heat carrier
Fo	Fourier number
Fr_M	modified Froude number
G	mass flowrate of heat carrier
G_1	mass flowrate of heat carrier before disturbing
G_2	mass flowrate of heat carrier after making disturbances
K	dimensionless effective turbulent diffusion coefficient
l	length
N	heat load
r	radial coordinate
r_{bundle}	radius of the tube bundle
Re	Reynolds number
s	twisting pitch of tubes
t	period of oscillations
T	temperature
u	velocity
x	longitudinal coordinate.

Greek symbols

ε	bundle porosity with respect to heat carrier
κ	relative mixing coefficient of heat carrier
λ	thermal conductivity
λ_{eff}	effective turbulent thermal conductivity
μ	dynamic viscosity coefficient
ν_{eff}	effective turbulent viscosity coefficient
ρ	density
τ	time.

Subscripts

b	bulk
f	fluid
m	mean
M	modified
max	maximum
min	minimum
p	at $p = \text{const}$
qs	quasi-steady
s	solid phase
un	unsteady.

The unsteady flow structure is also affected by the thermal inertia of tubes when cooled with a finite velocity resulting in additional heat release into the flow in the case of the heat carrier flowrate increase and $N = \text{const}$. A change of the unsteady effective turbulent diffusion coefficient K_{un} to its quasi-steady value K_{qs} occurring for ~ 10–12 s ceases after the measured and predicted temperatures at $K_{un} = K_{qs}$ have coincided (Fig. 1).

As the heat carrier flowrate sharply decreases with time and the heat load is constant ($N = \text{const}$), the measured heat carrier temperature at the fixed points of the flow core lies below the predicted one at $K = K_{qs}$ (Fig. 1). This is indicative of heat transfer enhancement in the helical tube bundle, as compared to the predicted value $K = K_{qs}$. This enhancement is attributable to the growth of the turbulence intensity in the time-dependent decelerating flow. The same effect is also seen in the flow with the favorable velocity gradient. The turbulence structure is also affected by the thermal inertia of tubes and by the inertia forces due to flow swirling responsible for the nonuniformity of volume force fields and the additional turbulization or the reduction of the turbulence level. As the flow decelerates with time, this effect also manifests itself in increasing the time of changing the unsteady coefficient K_{un} to its quasi-steady value K_{qs} when the Fr_M number decreases (Fig. 1).

When the heat carrier flowrate periodically varies with time and $N = \text{const}$, at the first time moments the initial conditions exert some influence on the time variation of the temperature fields and the coefficient K_{un}. This variation is expressed in a more strong deviation of these parameters from their quasi-steady values as against those in the regular regime when the variations of the temperature and the coefficient $\kappa = K_{un}/K_{qs}$ take the features of harmonic oscillations (Fig. 2) with the period t equal to that of flowrate fluctuations. In this case, the temperature minimum is shifted along the time axis by $0.25\ t$ with respect to the flowrate maximum. This is caused by the thermal inertia of tubes (Fig. 2), and the relative mixing coefficient κ undergoes periodic changes in back phase to the heat carrier flowrate.

The periodic change of the coefficient K_{un} (κ), by its nature, is similar to the changes of this coefficient when the flow accelerates and decelerates with time as the flowrate varies sharply [3]. However, because of the mutual influence of these processes in the periodic change of flowrate, the amplitude variation of the coefficient κ is smaller than in the case of the same ratio G_{max}/G_{min} (or G_{min}/G_{max}) when the flowrate varies

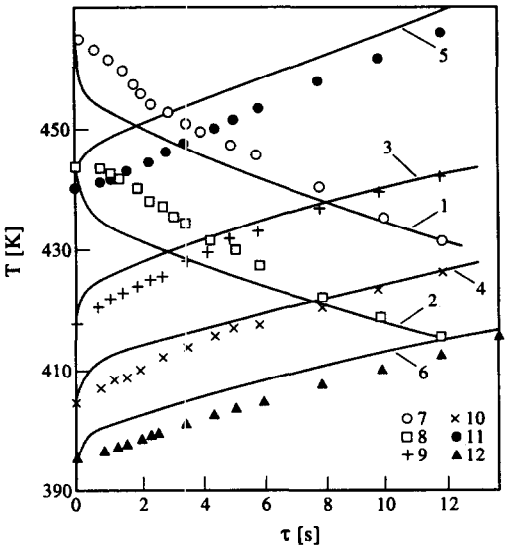

Fig. 1. Time variation of the experimental temperatures at different flow points and their comparison with the predicted ones in the quasi-steady approximation. (1, 2) calculation at $N = 59$ kW; $Fr_M = 220$; $G_2/G_1 = 1.71$ and $K_{qs} = 0.07$ for $r/r_{bundle} = 0.073$ and 0.264, respectively; (3, 4) calculation at $N = 7$ kW, $Fr_M = 220$, $G_2/G_1 = 0.611$ and $K_{qs} = 0.07$ for $r/r_{bundle} = 0.073$ and .264, respectively; (5, 6) calculation at $N = 7.5$ kW; $Fr_M = 57$; $G_2/G_1 = 0.605$ and $K_{qs} = 0.09$ $r/r_{bundle} = 0.073$ and 0.407, respectively; (7, 8) experiment at $N = 59$ kW; $Fr_M = 220$ and $G_2/G_1 = 1.71$; (9, 10) experiment at $N = 7$ kW; $Fr_M = 220$ and $G_2/G_1 = 0.611$; (11, 12) experiment at $N = 7.5$ kW; $Fr_M = 57$ and $G_2/G_1 = 0.605$.

sharply. As shown below, this variation of the coefficient κ is the smaller, the larger the frequency (the smaller t) and the smaller the fluctuation amplitude of the flowrate.

Figure 3 plots the results on transient processes in the helical tube bundle with simultaneous time variations of power and flowrate of heat carrier [4] as temperature dependences of heat carrier and tube wall at a given point of the flow core. The experimental temperatures are compared with the results of numerical computation of the system of the equations [1] with the dimensionless effective turbulent diffusion coefficient $K_{un} = K_{qs}$. A good coincidence of the experimental and predicted temperatures in this case is explained by the opposite influence both of the flow acceleration at $N = \text{const}$ when $K_{un} < K_{qs}$ and of the heat load growth at $G = \text{const}$ when $K_{un} > K_{qs}$ on the unsteady flow structure [2–5]. It may be assumed that when the heat load and flowrate increase simultaneously the equilibrium turbulence structure occurs during the entire transient process. The same situation is also seen when the heat load and heat carrier flowrate decrease simultaneously and the temperature and velocity profiles are invariable during the entire process (Fig. 3). In this case, when the flow decelerates in time and $N = \text{const}$ the coefficient $K_{un} > K_{qs}$ and when the heat load decreases and $G = \text{const}$ the coefficient $K_{un} < K_{qs}$ [2–5], i.e. when N and G decrease simultaneously these effects compensate each other and $K_{un} = K_{qs}$. This is illustrated by Fig. 3.

3. GENERALIZATION AND ANALYSIS OF THE EXPERIMENTAL DATA

As already noted, the comparison of the measured and predicted temperature fields of heat carrier allowed the coefficients K_{un} as well as the coefficients λ_{eff} and ν_{eff} to be determined for different types of unsteadiness. These coefficients are used to approximately close the system of the equations [1]. For the generalizing relations suitable for calculation of the dimensionless coefficient K_{un} to be obtained, the similarity and dimensionality theories were adopted. As a result, the following determining similarity numbers [2–5] were found:
the modified Froude number

$$Fr_M = S^2/dd_{eq} \tag{1}$$

characterizing the influence of swirling the flow on its transport properties;
the Fourier number

$$Fo_b = \frac{\lambda_b \tau}{c_p \rho_b d^2_{bundle}} \tag{2}$$

characterizing a relationship among the rate of varying the temperature of heat carrier, its physical properties and sizes of the flow region;
the Reynolds number

$$Re = \frac{u_m d_{eq} \rho}{\mu} \tag{3}$$

that slightly affects the coefficient K for $Re < 10^4$ [2].

For $Re \geqslant 10^4$ the coefficient K is self-similar with respect to the Reynolds numbers [2]. The influence of the variation of the heat carrier flowrate on the coefficient K_{un} was conveniently taken into account by the dimensionless parameter G_2/G_1 representing the ratio of the heat carrier flowrate after making disturbances (G_2) to the initial flowrate (G_1) [4, 5]. The coefficient K is also affected by the tube bundle porosity with respect to heat carrier $\varepsilon = F_f/F_\Sigma$ [2] where $F_\Sigma = F_f + F$. In this case, the criterial equation for determination of the unsteady coefficient K_{un} is of the form:

$$K_{un} = K(Fr_M, Fo_b, Re, G_2/G_1, \varepsilon). \tag{4}$$

To calculate the quasi-steady coefficient K_{qs}, we have the following functional relation [2]:

$$K_{qs} = K(Fr_M, Re, \varepsilon). \tag{5}$$

In generalizing the experimental data on unsteady mixing of heat carrier, the action of the factors that equally affect the coefficients K_{un} and K_{qs} may be excluded by introducing the relative mixing coefficient

$$\kappa = K_{un}/K_{qs} \tag{6}$$

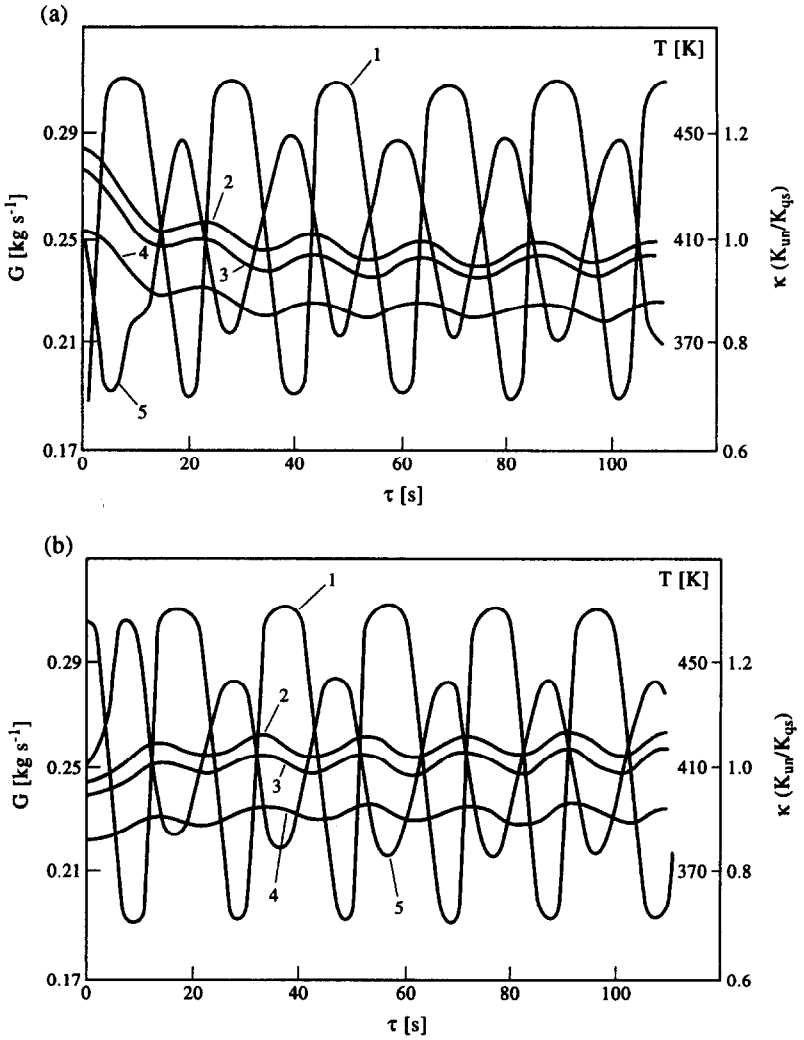

Fig. 2. Influence of the periodic time variation of heat carrier flowrate on the flow transport properties at $N = 7.1$ kW, $G_{max}/G_{min} = 1.625$ and at $t = 20$ s (a) and at $N = 7.7$ kW, $G_{min}/G_{max} = 0.62$ and $t = 20$ s (b): (1) time variation of flowrate; (2–4) time variation of temperature for $r/r_{bundle} = 0.073$, 0.193 and 0.334, respectively; (5) time variation of the relative coefficient $\kappa = K_{un}/K_{qs}$.

into consideration. This coefficient takes into account only the effects associated with the analyzed type of unsteadiness.

When the flow accelerates in time at $N = \text{const}$ the coefficient κ depends on the Fo_b number and the flowrate ratio G_2/G_1 (Fig. 4). In this case, the experimental data over the range of the flow parameters: $G_2/G_1 = 1.62$–1.77, $Re = 7 \cdot 10^3$–$1.2 \cdot 10^4$ and $Fr_M = 57$–220 are well generalized by the relations:

at $Fo_b = 0$–$4.5 \cdot 10^{-4}$

$$\kappa = 1 - 1.1364 \cdot 10^3 Fo_b \tag{7}$$

at $Fo_b = 4.5 \cdot 10^{-4} - 4.5 \cdot 10^{-2}$

$$\kappa = 4.04 Fo_b^n + \left[0.99 - 4.12\left(\frac{G_2}{G_1} - 1\right)^{3.8}\right] \tag{8}$$

where $n = 1.852 - 0.927(G_2/G_1)$. (9)

The proposed relations take into account the influence of these numbers responsible for the transfer process with a given type of unsteadiness in an explicit form and thus differ beneficially from the dependence considered in [5]:

$$\kappa = AFo_b^n + C \tag{10}$$

where A, C and n are the function of the flowrate ratio G_2/G_1. At the same time relations (8) and (10) correlate well (Figs 4 and 5).

As seen from Fig. 4, the coefficient κ decreases sharply at the first time moments. The time, for which the coefficient κ decreases sharply, is practically equal to that, for which the flowrate achieves a new regime (approximately 1 s). Such a change of the heat and momentum transfer coefficients can be first explained by the decrease of the turbulence intensity in the time-

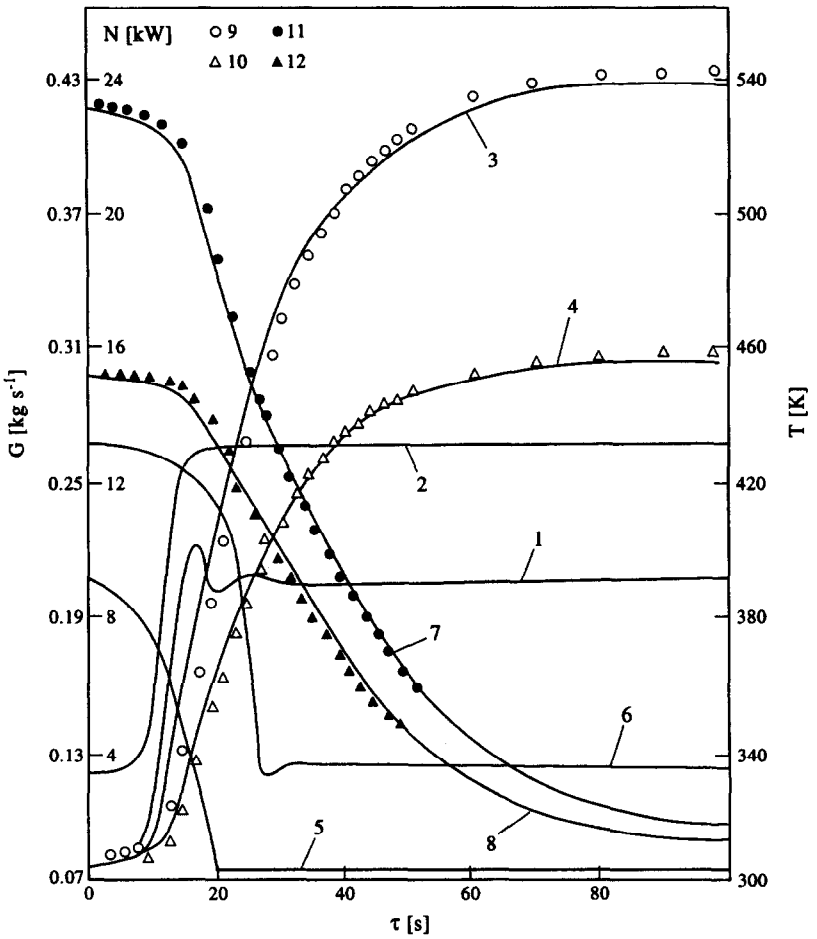

Fig. 3. Time variation of heat carrier and solid phase temperatures with simultaneous variation of heat power and flowrate at the point with the coordinates $x/l = 0.95$, $r/r_{bundle} = 0.073$. (1, 5) power variation; (2, 6) variation of heat carrier flowrate; (3, 4) predicted temperatures of the solid phase (T_s) and heat carrier (T) with simultaneous increase of N and G; (7, 8) the same with simultaneous decrease of N and G; (9, 10) experimentally measured temperatures T_s and T as N and G increase; (11, 12) the same as N and G decrease.

dependent accelerating flow. The coefficient κ then increases, gradually approaching $\kappa = 1$, while the time of this transition at $G_2 = \text{const}$ (τ) is approximately on the order of magnitude larger than that of the heat carrier flowrate achieving a new regime. After the flowrate G_2 has been set in, such a time variation of the coefficient κ can be affected mainly by the thermal inertia of the tubes when cooled, since the reconstruction of temperature fields, as well as the variation of temperature pulsations and thermal properties, and their correlations with velocity pulsations under the inertia forces due to flow swirling, will change the turbulence structure. The observed variability of the mean value of the density will be the cause of volume deformation of turbulent vorticies and will affect the turbulence characteristics. The coefficient K_{un} achieves its quasi-steady value far earlier than the heat carrier temperature attains its new steady value. This means that the temperature fields in helical tube bundles become similar in time, starting with $\kappa = 1$ (i.e. the shape of the temperature profiles becomes invariable in time).

Relations (8) and (10) show that the flow swirling does not affect the coefficient κ, i.e. the Fr_M number equally affects the unsteady (K_{un}) and quasi-steady (K_{qs}) transfer coefficients when the heat carrier flowrate increases at $N = \text{const}$. The larger the ratio G_2/G_1, the greater is the deviation of K_{un} from K_{qs}.

When the heat carrier flowrate decreases at $N = \text{const}$, the flow swirling exerts a more profound influence on the unsteady mixing mechanisms (Figs. 6 and 7) than in the case of time acceleration of the flow. In this case, as the swirling intensity grows (as the Fr_M number decreases), the time for which the coefficient K_{un} attains its quasi-steady value, increases. This can be explained by the fact that the unsteady flow structure is influenced by the additional action of the inertia forces due to the swirling intensity increase with decrease in the Fr_M number. Therefore, for this type of unsteadiness the generalizing relations

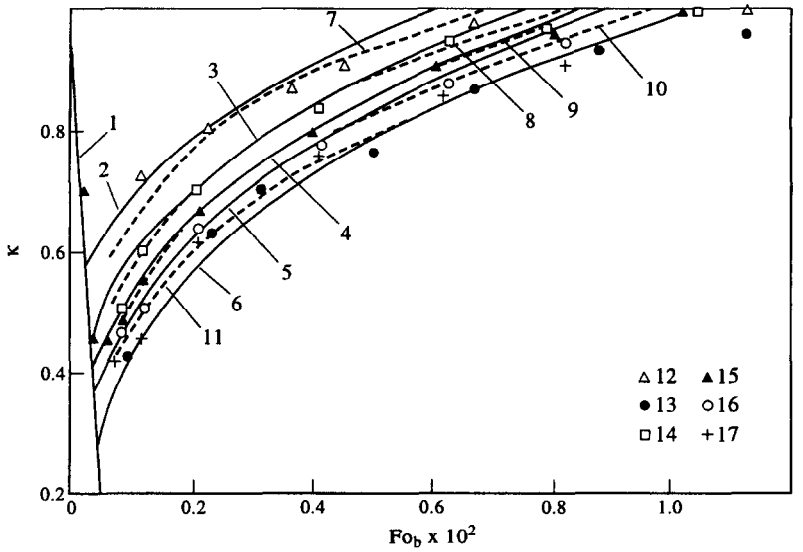

Fig. 4. Influence of time-dependent acceleration of the flow on its transport properties at different determining parameters. (1) relation (7); (2–6) relation (8) for the flowrate ratio $G_2/G_1 = 1.62$, 1.68, 1.71, 1.73 and 1.77, respectively; (7–11) relation (10) for $G_2/G_1 = 1.62$, 1.68, 1.71, 1.73 and 1.77; (12, 13) experiment for $Fr_M = 57$ and $G_2/G_1 = 1.62$ and 1.77, respectively; (14–17) the same for $Fr_M = 220$ and $G_2/G_1 = 1.68$, 1.71, 1.73 and 1.77, respectively.

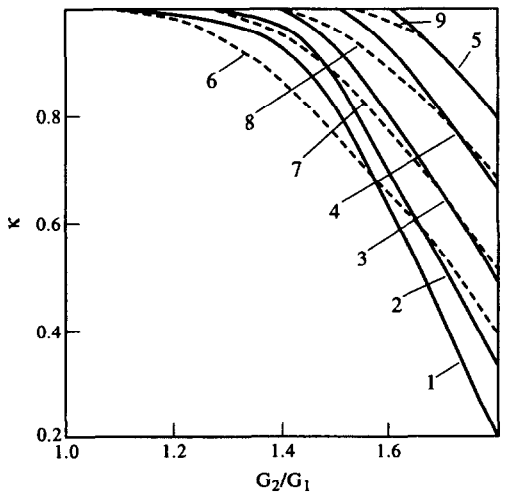

Fig. 5. Comparison of different generalizing relations for calculation of unsteady effective turbulent diffusion coefficient at flow acceleration. (1–5) relation (8) at $Fo_b = 5\cdot10^{-4}$, 10^{-3}, $2\cdot10^{-3}$, $4\cdot10^{-3}$ and $6\cdot10^{-3}$, respectively; (6–9) relation (10) for $Fo_b = 10^{-3}$, $2\cdot10^{-3}$, $4\cdot10^{-3}$ and $6\cdot10^{-3}$, respectively.

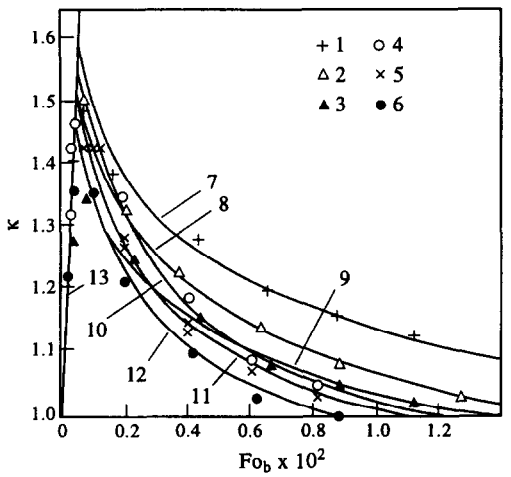

Fig. 6. Influence of time-dependent deceleration of the flow on its transport properties at different determining parameters (1-3) experiment at $Fr_M = 57$ and $G_2/G_1 = 0.665$ and 0.765, respectively; (4–6) experiment at $Fr_M = 220$ and $G_2/G_1 = 0.579$, 0.594 and 0.611, respectively; (7–9) relation (11) at $Fr_M = 57$ and $G_2/G_1 = 0.605$, 0.665 and 0.765; (10–12) relation (12) at $Fr_M = 220$ and $G_2/G_1 = 0.579$, 0.594 and 0.611; (13) relation (13).

were derived separately for each of the investigated helical tube bundles with $Fr_M = 57$ and 220 [5]. For the tube bundle with $Fr_M = 57$ the relation is of the form:

$$\kappa = (2.57\, Fo_b^{-0.0437} - 2.11) \times \left[2.95\cdot10^{-4}\left(\frac{G_2}{G_1}\right)^{-11.94} + 0.993\right]. \quad (11)$$

Formula (11) is valid at $Fo_b = 0.514\cdot10^{-3}$–$1.4\cdot10^{-2}$ and $G_2/G_1 = 0.605$–0.765. For the tube bundle with $Fr_M = 220$ the coefficient κ is determined by the relation:

$$\kappa = (0.398\, Fo_b^{-0.165} + 0.13)\left[0.645\left(\frac{G_2}{G_1}\right)^{-0.818} + 0.04\right] \quad (12)$$

valid at $Fo_b = 0.514\cdot10^{-3}$–$0.9\cdot10^{-2}$, $G_2/G_1 = 0.579$–0.611. A sharp increase of the coefficient κ at the first time moments at $Fo_b = 0$–$0.514\cdot10^{-3}$, $G_2/G_1 = 0.579$–

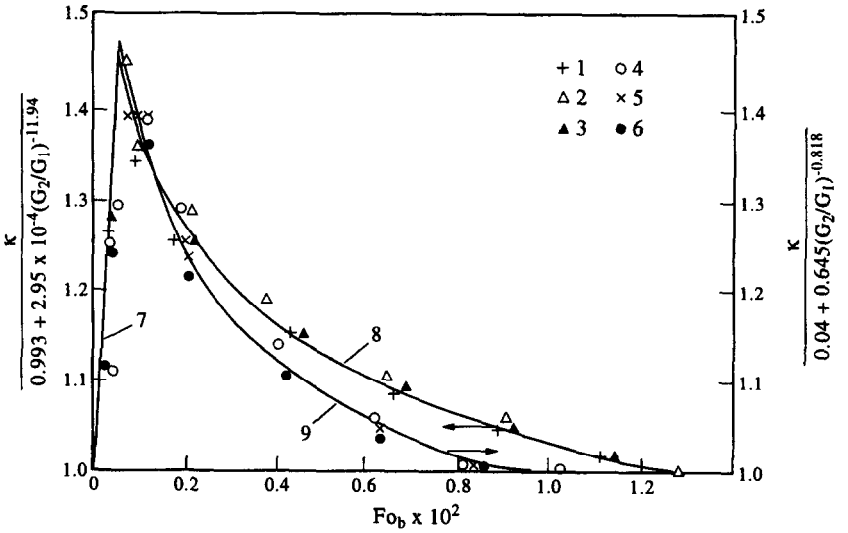

Fig. 7. Generalizing relations for flow deceleration. (1–3) experiment at $Fr_M = 57$ and $G_2/G_1 = 0.605, 0.665$ and 0.765; (4–6) experiment at $Fr_M = 220$ and $G_2/G_1 = 0.579$, 0.594 and 0.611; (7) relation (13); (8) relation (11); (9) relation (12).

0.765 for the tube bundles with $Fr_M = 57$ and 220 is governed by the same relation

$$\kappa = (1 + 927\, Fo_b)\left[2.95 \cdot 10^{-4}\left(\frac{G_2}{G_1}\right)^{-11.94} + 0.993\right]. \tag{13}$$

Along with relations (11) and (12) for calculation of the coefficient κ, the formulas can be proposed, which are similar in structure to relation (8) and are of the following form for the tube bundles $Fr_M = 57$ and 220, respectively:

$$\kappa = 2.57 Fo_b^{0.009(G_2/G_1)-0.049} - \left[1.488 + 0.8125\left(\frac{G_2}{G_1}\right)\right] \tag{14}$$

$$\kappa = 0.391\, Fo_b^{0.1875(G_2/G_1)-0.278} + \left[1.085 - 1.56\left(\frac{G_2}{G_1}\right)\right]. \tag{15}$$

Formulas (14) and (15) adequately describe the experimental data on the coefficient κ and allow it to be plotted as a function of Fourier number and flowrate ratio in a more simple form (Figs. 8–11).

As already noted, a sharp increase of the coefficient κ at the first time moments can be explained mainly by the growth of the turbulence intensity in the time-dependent decelerating flow. The time, for which the coefficient κ reaches its maximum value, corresponds to that, for which the flowrate attains its now steady value of G_2. In what follows, the coefficient κ tends to unity (the coefficient K_{un} approaches K_{qs}). The behavior of the coefficient K_{un} at $G_2 = \text{const}$ is mainly influenced by the thermal inertia of the tubes when heated, which causes heat carrier temperature fields to reconstruct the mean density of heat carrier to vary with time. When acted on by the inertia forces, this reduces the turbulence intensity and compensates its initial growth due to flow deceleration with time. The coefficient K_{un} attains its quasi-steady value far earlier before a new temperature regime of the tube bundle has been set in. Starting with the moment corresponding to the time, for which the coefficient K_{un} reaches its quasi-steady value ($K_{un} = K_{eq}$), the temperature fields in helical tube bundles become similar in time.

When the heat carrier flowrate varies periodically the unsteady coefficient K_{un} varies approximately with the same rate as the flowrate does. However, the oscillation amplitude of the quantity $\kappa = K_{un}/K_{eq}$ at the first time moments is larger than that of κ, while

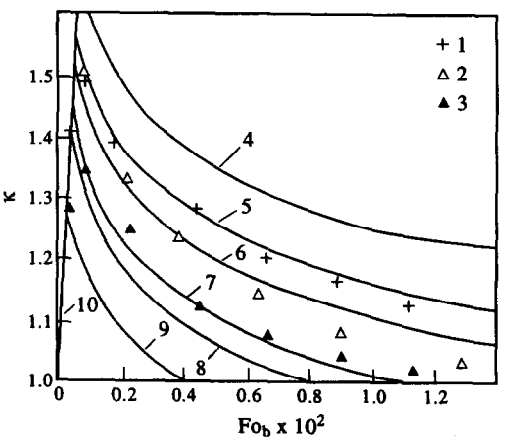

Fig. 8. Comparison of the experimental data on time deceleration of the flow at $Fr_M = 57$ with relation (14). (1–3) experiment at $G_2/G_1 = 0.605$, 0.665 and 0.765; (4–9) calculation by formula (14) at $G_2/G_1 = 0.5, 0.605, 0.665, 0.765$, 0.8 and 0.9, respectively; (10) relation (13).

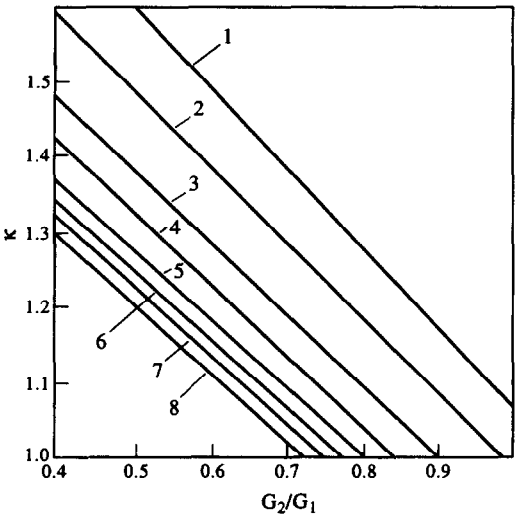

Fig. 9. Coefficient κ vs flowrate ratio G_2/G_1 for $Fr_M = 57$. (1–8) calculation by formula (14) at $Fo_b = 10^{-3}$, $2\cdot10^{-3}$, $4\cdot10^{-3}$, $6\cdot10^{-3}$, $8\cdot10^{-3}$, 10^{-2}, $1.2\cdot10^{-2}$ and $1.4\cdot10^{-2}$, respectively.

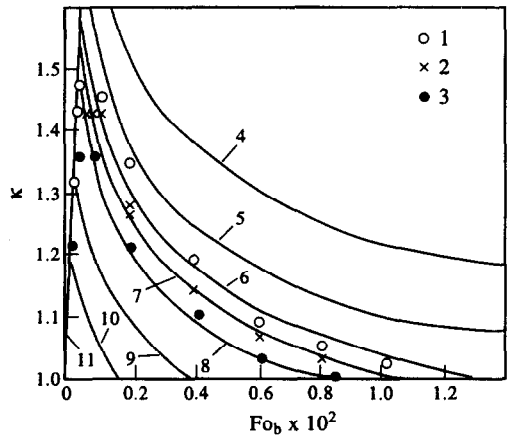

Fig. 10. Comparison of the experimental data on time deceleration of the flow at $Fr_M = 220$ with relation (15). (1–3) experiment at $G_2/G_1 = 0.579$, 0.594 and 0.611, respectively; (4–10) calculation by formula (15) at $G_2/G_1 = 0.5$, 0.55, 0.579, 0.594, 0.611, 0.65 and 0.7, respectively; (11) relation (13).

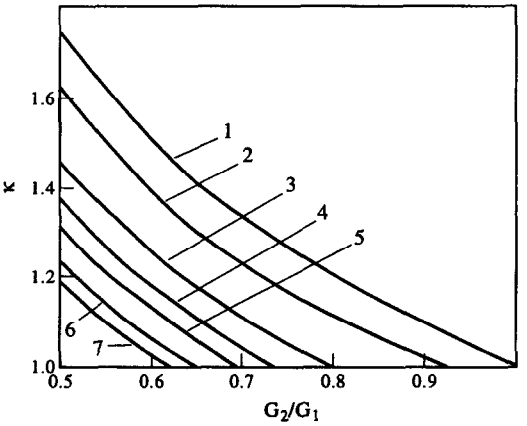

Fig. 11. Coefficient κ vs flowrate ratio G_2/G_1 for $Fr_M = 220$. (1–7) calculation by formula (15) at $Fo_b = 5\cdot10^{-4}$, 10^{-3}, $2\cdot10^{-3}$, $3\cdot10^{-3}$, $4\cdot10^{-3}$, $6\cdot10^{-3}$ and $8\cdot10^{-3}$, respectively.

reaching the regular regime (Fig. 2) when the oscillation amplitude of the flowrate is kept invariable during the entire process. In passing from the steady-state operating conditions of the helical tube bundle to those involving a periodic variation of the flowrate due to the influence of the initial conditions at the initial time moments, the temperature and the coefficient κ vary in the same manner as in the case of a sharp flowrate variation. This influence of the initial conditions is seen for 1.5–2 oscillation periods. In this case, for the equal values of the ratios G_2/G_1, when the flowrate varies periodically, a maximum deviation of κ from unity is approximately by 25% less than in the case of a sharp variation of flowrate. In reaching a regular oscillation regime the amplitude of the quantity κ is approximately two times smaller than in the case of a sharp variation of flowrate. This behavior of κ evidences that it is affected by the main characteristics of the periodic time variation of flowrate: amplitude and period (frequency) of oscillations.

The conducted investigations have shown that when the flowrate ratios $G_{max}/G_{min} = \text{const}$ and the oscillation frequencies increase (the period t decreases), the oscillation amplitudes of the heat carrier temperature and, hence, of the coefficient κ decrease. So, for the flowrate variation periods $t = 70$, 50, 20 and 12.5 s the temperature amplitude constituted ±17, ±13, ±6 and ±3°C within the regular oscillation regime, i.e. increasing the flowrate oscillation frequency at a constant amplitude smooths the time variation of temperature and, hence, of κ. For the oscillation periods ($t \leqslant 4$ s) the influence of this type of unsteadiness on heat carrier temperature fields can be ignored.

The value of the amplitude of sinusoidal flowrate oscillations with time also much affects the coefficient κ. So, for the flowrate oscillation amplitude over the range $\Delta G/G_m = \pm0.25$–±0.35 the coefficient κ varies within 0.8–1.2 at $\Delta G/G_m = \pm0.15$–0.25, $\kappa = 0.9$–1.1 and at $\Delta G/G_m < \pm0.15$ $\kappa \approx 1$, i.e. the influence of this type of unsteadiness can be neglected.

4. CONCLUSIONS

(1) A method of closing a system of equations for flow and heat transfer in complex-geometry channels is developed and is based both on the hypothesis for similarity of transfer processes and on the mathematical formalism to solving the unsteady thermohydraulic problem.

(2) The established new mechanisms of unsteady mixing of heat carrier, when the heat carrier flowrate decreases and increases and varies periodically with time, can be utilized for calculation of effective turbulent thermal conductivity and viscosity coefficient in complex-geometry channels with flow swirling.

(3) The revealed effects influencing heat transfer with time variation of heat carrier flowrate allow one to explain the physical nature of transfer processes

which are governed by the established relations for different types of unsteadiness.

REFERENCES

1. Dzyubenko, B. V., Dreitser, G. A. and Kalyatka, A. V., Mechanisms of unsteady mixing of heat carrier with its flowrate variation and flow swirling—I. Calculation methods and experimental study of transient processes. *International Journal of Heat and Mass Transfer* 1998, **41**, 645–651.
2. Dzyubenko, B. V., Dreitser, G. A. and Ashmantas, L.-V. A., *Unsteady Heat and Mass Transfer in Helical Tube Bundles*. Hemisphere, New York, 1990.
3. Dzyubenko, B. V., Ashmantas, L.-V. A., Bagdonavichyus, A. B. and Kalyatka, A. V., Interchannel mixing of heat carrier with its periodic variation of flowrate in helical tube bundles. *J. Engng Phys.*, 1991, **60**(5), 724–729.
4. Dzyubenko, B. V., Bagdonavichyus, A. B., Kalyatka, A. V. and Segal, M. D., Unsteady heat and mass transfer with simultaneous variations of heat power and flowrate of heat carrier. *J. Engng Phys.*, 1992, **62**(3), 349–355.
5. Dzyubenko, B. V., Ashmantas, L.-V. A. and Segal, M. D., *Modelling of Steady and Transient Thermal and Hydraulic Processes in Complex-Geometry Channels*. Pradai, Vilnius, 1994.